Canadian Mineralogist
Vol. 26, pp. 1013-1025 (1988)

THE LAC-ST-JEAN ANORTHOSITE IN THE ST-HENRI-DE-TAILLON AREA (GRENVILLE PROVINCE): A RELIC OF A LAYERED COMPLEX

GÉRARD WOUSSEN
Sciences de la terre, Université du Québec à Chicoutimi, Chicoutimi, Québec G7H 2B1

JACQUES MARTIGNOLE
Département de Géologie, Université de Montréal, C.P. 6128, Montréal, Québec H3C 3J7

SUZIE NANTEL
Ministère de l'Énergie et des Ressources du Québec, 1620, boulevard de l'Entente, Québec, Québec G1S 4N6

Abstract

The Lac-St-Jean anorthosite massif underlies 20,000 km^2 of the "Allochthonous Polycyclic Belt" of the Grenville Province in Quebec. This heterogeneously deformed massif was emplaced during a major extensional episode that predated the Grenvillian Orogeny. In the southwestern part of the massif, an almost undeformed subcircular layered complex about 10 km in diameter was identified and subdivided into four major units. This complex, which shows strong similarities with the anorthosite massifs of the Nain and Churchill provinces, consists largely of variable amounts of anorthosite and leucotroctolite interlayered at a decimetric to decametric scale. The rocks consist predominantly of large homogeneous cumulus plagioclase ($\sim An_{60}$) and of six intercumulus minerals: reversely zoned plagioclase (An_{59-83}), olivine ($\sim Fo_{69}$), minor amounts of orthopyroxene ($\sim En_{72}$), clinopyroxene ($\sim Wo_{45}En_{44}$), Fe–Ti oxide minerals and apatite. No significant cryptic layering was observed from the bottom to the top of the suite, possibly implying that only a small part of a huge layered complex is exposed. The near-cotectic proportions of plagioclase and olivine suggest that the intercumulus material represents a trapped liquid composition that crystallized isobarically. The magma and its entrained plagioclase are thought to have originated at the crust–mantle interface.

Keywords: Grenville Province, Lac St-Jean, anorthosite, leucotroctolite, layering, mineralogy, plagioclase, orthopyroxene, clinopyroxene, olivine.

Sommaire

Le massif d'anorthosite du Lac-St-Jean (Québec) occupe une superficie de 20 000 km^2 de la "Ceinture Polycyclique Allochtone" de la province du Grenville. Ce massif, qui est déformé de façon hétérogène, s'est mis en place durant une période d'extension crustale majeure qui a précédé l'orogénie grenvillienne. Dans la partie sud-ouest du massif, un complexe stratiforme d'environ 10 km de diamètre a été identifié et subdivisé en quatre unités majeures. Ce complexe, analogue à ceux des provinces de Nain et de Churchill, contient essentiellement des roches anorthositiques et leucotroctolitiques en bancs décimétriques et décamétriques. Ces roches ont une minéralogie simple: plagioclase cumulus en cristaux de grande taille ($\sim An_{60}$) et minéraux intercumulus. Dans un ordre d'abondance décroissant, les minéraux intercumulus sont: plagioclase inversement zoné (An_{50-83}), olivine ($\sim Fo_{69}$), orthopyroxène ($\sim En_{72}$), clinopyroxène ($\sim Wo_{45}En_{44}$), oxydes de Fe–Ti et apatite. Aucun litage cryptique ne fut observé de la base de la suite vers le sommet; ceci indique vraisemblablement que nous sommes en présence d'une partie seulement d'un vaste complexe stratiforme. La fraction précipitée entre les cristaux de plagioclase cumulus montre une proportion quasi-cotectique d'olivine et de plagioclase. La fraction intercumulus représenterait donc la composition du liquide interstitiel, qui a cristallisé de façon isobare. Le magma initialement enrichi en cristaux de plagioclase émane probablement de l'interface croûte–manteau.

Mots-clés: province du Grenville, Lac St-Jean, anorthosite, leucotroctolite, litage, minéralogie, plagioclase, orthopyroxène, clinopyroxène, olivine.

Introduction

The Lac-St-Jean anorthosite (LSJA) massif, located in the Saguenay – Lac-St-Jean area of Quebec, covers an area of about 20,000 km^2 (Fig. 1). It may be a large composite pluton, consisting of several cogenetic and layered intrusive units of as yet unknown dimensions; subsequent deformation and subsolidus evolution have obscured many of its magmatic features. In common with many anorthosite massifs of the Grenville Province, no mafic or ultramafic units have been observed at the base of the LSJA massif; the negative gravity anomaly over the massif (Gravity Division Map, 1974) suggests that no such rocks are present at depth.

The tectonic setting of most anorthosite massifs of the Grenville Province is still poorly understood, and so is their time of emplacement. Similarities and differences with the layered anorthosite of the Churchill and Nain provinces are still incompletely documented. However, the presence of widespread post-Hudsonian amphibolite dyke-swarms in the

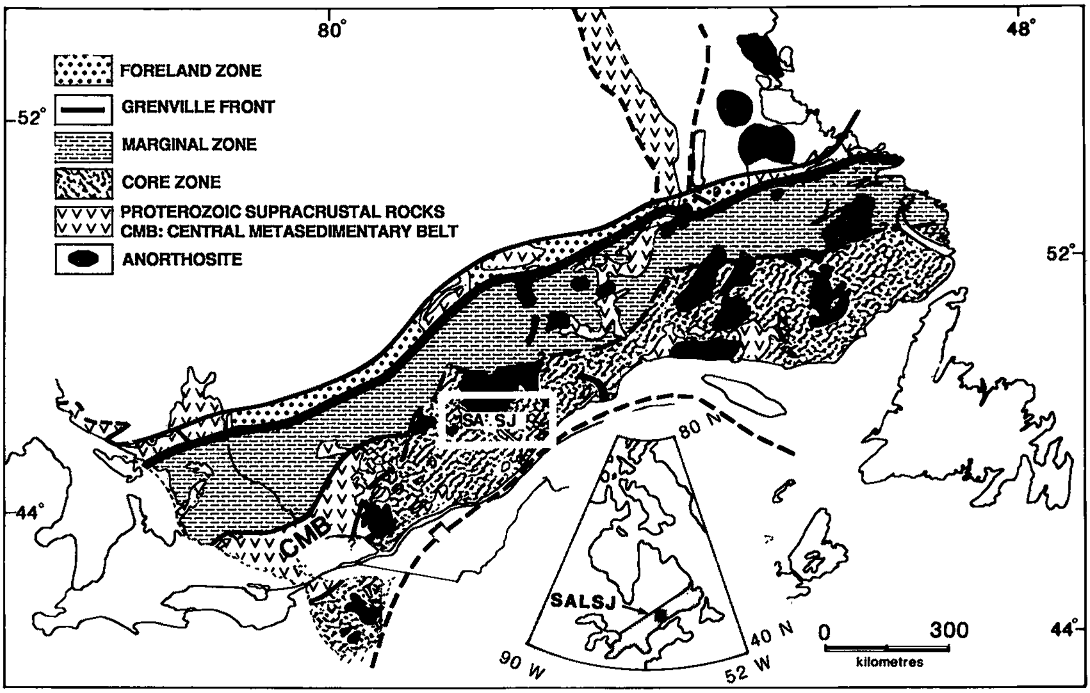

FIG. 1. Geotectonic subdivisions of the Grenville Province and location of the Saguenay - Lac-St-Jean area (SALSJ),

gneiss complex surrounding the LSJA massif indicates a major Pre-Grenvillian episode of crustal extension, tentatively ascribed to the Elsonian (*ca.* 1450 Ma) intrusive episode (Woussen *et al.* 1981, 1986, Dimroth *et al.* 1981). The close association of the LSJA massif with metamorphosed mafic dykes suggests that both may be related to the same magmatic episode.

Except for some detailed mapping in regions located more than 100 km to the northeast (Kehlenbeck 1972a, b, Hocq 1977), there is little information available about the LSJA massif. The majority of the areas pertaining to this work have been mapped only at a scale of 1:250,000 (Laurin & Sharma 1975). However, mapping in the southwestern part of the massif, at a scale of 1:20,000 (Nantel *et al.* 1985), has revealed the presence of well-preserved, largely undeformed segments of a rhythmically layered sequence of anorthosite - leucotroctolite rocks (Fig. 2).

The major rock-units in the St-Henri-de-Taillon area, part of this undeformed segment, are described briefly in this paper; as well, quantitative data on the premetamorphic textural and chemical characteristics of the magmatic minerals are given. This information forms a basis for further studies in other parts of the LSJA, where the mineralogy and textures of the rocks have been significantly modified by deformation and subsolidus reactions among minerals. The information also provides clues to the genesis of similar types of anorthosite massifs elsewhere in the Grenville Province. Finally, the quantitative data presented here represent the first detailed account of premetamorphic mineral textures and compositions from the LSJA massif, often considered to be the largest in the world.

GEOLOGICAL SETTING

The LSJA is located in the "Allochthonous Polycyclic Belt" of Rivers *et al.* (1989), which is equivalent in part to the "Core Zone" (Woussen *et al.* 1986) of the Grenville Province (Fig. 1). The stratigraphic column for the surrounding gneiss complex is presented in Figure 3.

Schematically, the Precambrian rocks of the Saguenay - Lac-St-Jean area may be described in terms of three major lithostructural units: i) a gneiss complex comprising: a) complexly deformed and migmatized quartzofeldspathic gneisses of unknown age, b) rafts of Aphebian metasediments, c) deformed late- to post-Hudsonian granites (*ca.* 1700 Ma), and d) deformed and segmented major amphibolite dyke-swarms, which cut the earlier rock-

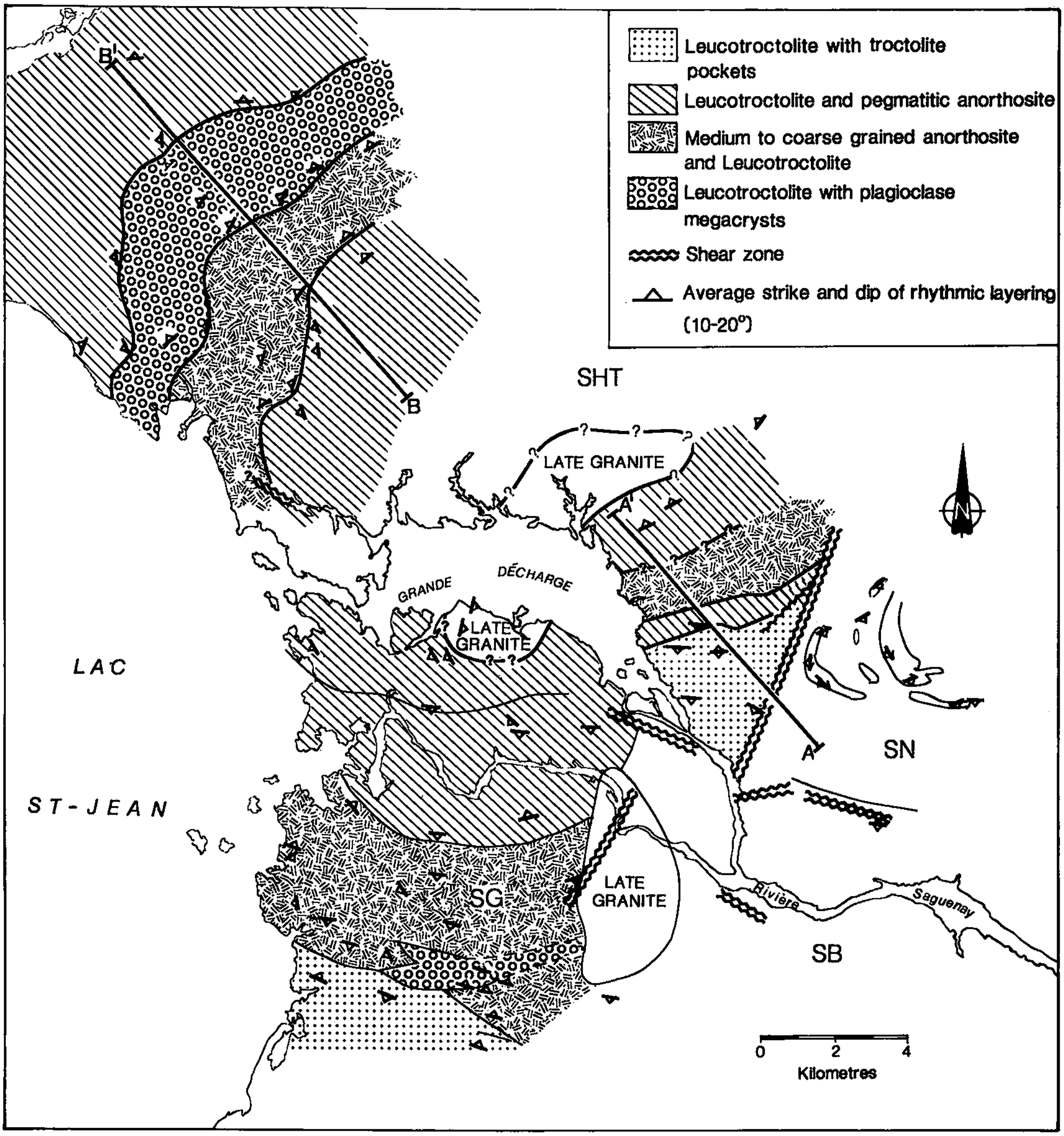

FIG. 2. Rock units of the southwestern part of the Lac-St-Jean anorthosite massif. Analyzed samples are close to traverses AA′ and BB′. SHT: St-Henri-de-Taillon block; SG: St-Gédéon block; SN: St-Nazaire block, SB: St-Bruno Block. Tectonic blocks SN and SB consist of interlayered gneissic leuconorite and leucotroctolite.

units; ii) large anorthosite – mangerite (charnockite) plutons that cut the gneiss complex, and iii) relatively smaller late- to post-Grenvillian hornblende and biotite granite exhibiting a calc-alkaline differentiation trend (Roy *et al.* 1986). During the Grenvillian orogeny (1200–1000 Ma), the two older units were variously remobilized.

GEOLOGY OF THE SOUTHWESTERN PART OF THE LSJA MASSIF

Two major belts of ductile deformation are observed in the southwestern part of the LSJA massif. These belts, which strike east–west and northeast–southwest, have dissected this part of the

PROTEROZOIC	NEOHELIKIAN	Dykes	-Diabase and basic rocks
		Anorthosite	-St Nazaire anorthosite
		Late Granites	-Pegmatites -Porphyritic granites -Alaskite
	GRENVILLE OROGENY ~1.2 Ga		
	PALEO-HELIKIAN	Granitoids	-Mangerite, charnockite
		Lac St-Jean anorthosite	-Anorthosite, Leucotroctolite, Leuconorite, Troctolite, Norite
		Amphibolite	-Amphibolite ‖ dykes
		Granitoids	-Hornblende and pink feldspar bearing mixed green rocks
	HUDSONIAN OROGENY ~1.7 Ga		
	APHEBIAN	Quartzo-feldspathic gneisses and Metasediments	-Mixed gneiss and banded gneiss -Grey gneiss -Amphibolite -Sillimanite-cordierite-garnet gneiss -Quartzite -Calcsilicate gneiss

FIG. 3. Relative chronological succession of the lithologies in the gneiss complex west of the Lac-St-Jean anorthosite massif (modified from Benoit & Valiquette 1971).

massif into four tectonic blocks, here referred to as the St-Henri-de-Taillon, St-Gédéon, St-Nazaire, and St-Bruno blocks (Fig. 2).

The St-Henri-de-Taillon and the St-Nazaire blocks, which are north of the Saguenay River, are separated from the St-Gédéon - St-Bruno blocks by a subvertical and approximately east–west belt of gneissic anorthosite up to 1.5 km wide, in which are mylonites locally up to 40 m in width. This belt of high-strain rocks is broadly parallel to the Saguenay River (Fig. 2).

A zone of intense deformation, about 0.5 km in width and characterized by local subvertical north-northeast ductile shears, separates the western blocks from the St-Nazaire - St-Bruno blocks to the east (Fig. 2). This tectonic zone marks a transition between the relatively undeformed western blocks and the more strongly deformed and recrystallized eastern blocks. The eastern blocks, characterized by interlayered rocks where orthopyroxene and olivine alternate as the dominant intercumulus phase, differ mineralogically from the rocks of the St-Henri-de-Taillon and St-Gédéon (western) blocks, where olivine is the only important postcumulus mineral (Fig. 2). However, as shown in Figure 2, gently dipping layering in the western blocks (St-Henri-de-Taillon - St-Gédéon regions) defines a subcircular domical pattern about 10 km in diameter. This largely undeformed complex consists of anorthosite and leucotroctolite interlayered on the centimeter to the decameter scale. Apart from local deformation, the St-Henri-de-Taillon segment is probably the least deformed of the southern part of the LSJA massif. The St-Gédéon block has the same general traits, but its mineralogy has been modified significantly at several places by the emplacement of syn- and late-tectonic granitic plutons (Fig. 2) and numerous pegmatite dykes.

DESCRIPTION OF THE ROCK UNITS IN THE ST-HENRI-DE-TAILLON BLOCK

The St-Henri-de-Taillon block is divided into four units whose thicknesses range from about 500 to 1000 m. The units are defined on the basis of texture, plagioclase–olivine ratio and, to a lesser extent, the degree of deformation (Fig. 2). The succession shows, in almost pristine condition, some of the structures and textures typical of stratiform complexes of the upper crust, or of anorthosite massifs of the Churchill and Nain provinces (*e.g.*, the Harp Lake complex: Emslie 1980).

Layering is omnipresent and generally consists of layers that range in thickness from a few centimeters to several meters. The repetition of light and dark layers results largely from differing amounts (2% to 30%) of intercumulus olivine. As olivine, except locally, is only a postcumulus phase, the rhythmic succession corresponds to a modal layering (Irvine 1982). The contacts between the layers are sharp, but lateral continuity of the layering does not persist for more than a few meters or tens of meters. In some cases, the term *lenses* (of layered rocks) would be more appropriate to describe the structure. Similar laterally discontinuous layers were observed in the Harp Lake complex of the Churchill Province (Emslie 1980) and locally in the Stillwater complex (McCallum *et al.* 1980). Planar lamination (Jackson 1967) is common and results from the orientation of (010) faces of platy plagioclase crystals parallel to modal layering. Where the rocks are deformed, shearing is parallel to the igneous lamination, and the mafic minerals are stretched along the planes of shearing or flattening.

In some layers, 50 cm to 5 m thick, the intercumulus material is segregated into small leucotroctolitic or troctolitic ovoid pockets 5 to 15 cm in diameter. Locally, the quantity of ovoid pockets increases; where they coalesce, they give a patchy appearance to the rock surface. These ovoid pockets, which are common in anorthosite massifs, are either (leuco)troctrolitic or (leuco)noritic in composition. They have been interpreted either as features of late crystallization (de Waard & Romey 1969, Maquil & Duchesne 1984) or as mafic mobilizates (Michot & Michot 1969).

TABLE 1. CHARACTERISTIC COMPOSITIONS OF THE MINERALS FROM THE ST-HENRI-DE-TAILLON COMPLEX

SAMPLE NO	A4-01F03A				G5-02B02A					G9-04B03A				
MINERAL	PL-C	OL	OPX	CPX	PL-C	PL-I	OL	OPX	CPX	PL-C	PL-I	OL	OPX	CPX
SIO2	54.31	37.35	53.20	51.16	53.69	50.43	37.51	53.77	51.07	52.06	52.00	37.49	53.12	51.11
AL2O3	28.45	0.02	2.04	3.32	29.78	31.37	0.02	2.06	3.41	29.04	29.37	0.01	1.98	3.32
TIO2	0.03	0.02	0.16	0.66	0.03	0.02	0.01	0.08	0.65	0.02	0.03	0.02	0.15	0.66
FEO(T)	0.08	29.07	17.43	6.55	0.12	0.18	29.32	17.47	6.76	0.12	0.13	29.80	17.51	6.73
MNO	0.02	0.45	0.42	0.22	0.01	0.01	0.37	0.33	0.16	0.03	0.02	0.43	0.36	0.18
MGO	0.01	33.91	26.16	14.69	0.05	0.03	34.48	26.33	14.59	0.01	0.00	34.79	26.72	14.98
CAO	11.21	0.00	0.57	22.56	12.20	14.35	0.02	0.51	22.27	12.47	12.76	0.01	0.60	22.50
NA2O	4.71	0.02	0.05	0.52	4.38	3.05	0.02	0.02	0.41	4.17	4.05	0.01	0.02	0.40
K2O	0.23	0.00	0.00	0.00	0.23	0.12	0.01	0.01	0.00	0.20	0.19	0.01	0.01	0.00
CR2O3	0.00	0.00	0.00	0.10	0.00	0.01	0.00	0.02	0.03	0.01	0.00	0.00	0.00	0.02
F	ND				0.04	ND				ND	ND			
CL	ND				0.01	ND				ND	ND			
TOTAL	99.05	100.84	100.03	99.78	100.54	99.57	101.76	100.60	99.35	98.13	98.55	102.57	100.47	99.90
NUMBERS OF IONS (*10000)	32"O"	4"O"	6"O"	6"O"	32"O"	32"O"	4"O"	6"O"	6"O"	32"O"	32"O"	4"O"	6"O"	6"O"
SI	98864	9957	19365	19003	96672	92042	9913	19435	19032	96196	95724	9853	19268	18963
AL4+	61036	5	634	997	63172	67536	6	565	967	63244	63720	2	732	1037
AL6+		0	241	456				311	530				114	414
TI	40	4	44	184	47	26	2	21	184	24	44	4	40	184
FE	116	6482	5306	2034	182	277	6480	5280	2107	180	204	6550	5311	2088
MN	36	101	129	69	9	19	84	101	52	44	36	95	110	56
MG	24	13476	14193	8133	128	92	13584	14184	8103	24	8	13630	14446	8284
CA	21860	0	222	8978	23536	28591	5	195	8893	24700	25164	4	233	8944
NA	16620	11	35	374	15292	10795	10	5	298	14932	14460	4	14	287
K	536	2	0	0	536	279	3	1	2	468	448	3	4	0
CR	4	1	0	29	7	15	1	5	8	20	0	0	0	5
F	—				214	—				—	—			
CL	—				10	—				—	—			
TOTAL	199136	30039	40169	40257	199804	199672	30088	40103	40178	199832	199808	30145	40272	40262
	OR 1.38		WO 1.11	WO 46.73	OR 1.37	OR 0.71		WO 0.99	WO 46.22	OR 1.16	OR 1.12		WO 1.07	WO 46.16
	AB 42.59	FO 67.18	FS 27.38	FS 10.95	AB 38.85	AB 27.19	FO 67.58	FS 27.23	FS 11.27	AB 37.24	AB 36.10	FO 67.23	FS 26.98	FS 11.09
	AN 56.03	FA 32.82	EN 71.50	EN 42.32	AN 59.79	AN 72.11	FA 32.42	EN 71.79	EN 42.30	AN 61.60	AN 62.78	FA 32.77	EN 71.86	EN 42.75
WOOD & BANNO C			853					885					876	
WELLS C			825					868					856	

SAMPLE NO	4E-29592TT					3E-29592/					6G-29498D				
MINERAL	PL-C	PL-I	OL	OPX	CPX	PL-C	PL-I	OL	OPX	CPX	PL-C	PL-I(*)	OL	OPX	CPX
SIO2	53.92	50.26	38.08	53.56	52.20	50.93	50.86	38.09	53.79	51.48	53.00	52.23	37.48	54.08	51.86
AL2O3	29.27	30.95	0.00	2.31	2.76	27.89	30.27	0.01	2.42	3.82	28.90	29.42	0.00	1.88	2.15
TIO2	0.01	0.01	0.01	0.14	0.37	2.45	0.02	0.01	0.20	0.74	0.01	0.03	0.00	0.08	0.31
FEO(T)	0.11	0.27	27.15	16.36	5.81	1.78	0.08	28.45	16.98	6.60	0.16	0.09	26.57	16.44	5.85
MNO	0.02	0.01	0.29	0.33	0.15	0.01	0.01	0.40	0.28	0.16	0.01	0.00	0.37	0.36	0.17
MGO	0.01	0.04	36.47	26.89	15.36	0.33	0.01	34.51	26.54	14.81	0.01	0.00	34.95	27.20	15.59
CAO	12.32	14.48	0.01	0.63	23.33	11.14	14.03	0.02	0.54	22.54	12.40	12.88	0.01	0.43	23.02
NA2O	4.32	3.11	0.03	0.02	0.36	4.51	3.62	0.02	0.00	0.44	4.30	3.96	0.02	0.02	0.34
K2O	0.23	0.10	0.01	0.01	0.01	0.87	0.09	0.01	0.01	0.01	0.29	0.19	0.00	0.00	0.00
CR2O3	0.01	0.01	0.01	0.02	0.01	0.02	0.01	0.00	0.01	0.00	0.01	0.01	0.03	0.01	0.01
F	0.00	ND				0.00	ND				0.00	ND			
CL	0.00	ND				0.00	ND				0.00	ND			
TOTAL	100.21	99.24	102.06	100.27	100.36	99.91	99.00	101.52	100.77	100.60	99.05	98.81	99.43	100.50	99.30
	32"O"	32"O"	4"O"	6"O"	6"O"	32"O"	32"O"	4"O"	6"O"	6"O"	32"O"	32"O"	4"O"	6"O"	6"O"
SI	97302	92324	9944	19336	19201	93786	93554	10035	19354	18933	96976	95840	10017	19466	19295
AL4+	62322	67044	0	664	799	60514	65623	4	645	1066	62316	63620	0	534	705
AL6+				319	401			0	381	589			0	264	237
TI	14	24	3	39	104	3424	27	2	54	204	10	44	1	21	86
FE	160	404	5929	4939	1789	2774	1	6268	5109	2031	238	144	5938	4951	1821
MN	36	15	64	103	46	16	15	89	85	49	12	0	83.00	101.00	53.00
MG	8	124	14096	14467	8423	912	27	13551	14234	8118	28	0	13923	14593	8645
CA	23831	28534	5	246	9194	21963	27650	6	208	8882	24296	25340	3	165	9176
NA	15111	11052	16	17	257	16108	12911	10	0	311	15234	14092	11	14	245
K	532	215	1	2	5	2056	211	3	4	4	662	448	0	1	1
CR	8	7	1	5	2	26	14	10	2	1	8	20	6	2	2
F	0	—				—	—				—	—			
CL	0	—				—	—				—	—			
TOTAL	199324	199743	30059	40137	40221	201579	200033	29978	40076	40188	199780	199548	29982	40112	40266
	OR 1.35	OR 0.54		WO 1.24	WO 47.26	OR 5.17	OR 0.52	FO 67.18	WO 1.05	WO 46.55	OR 1.65	OR 1.13		WO 0.83	WO 46.59
	AB 38.29	AB 27.76	FO 70.20	FS 25.52	FS 9.50	AB 40.15	AB 31.66	FA 32.82	FS 26.46	FS 10.90	AB 37.84	AB 35.36	FO 69.81	FS 25.52	FS 9.51
	AN 60.37	AN 71.69	FA 29.80	EN 73.23	EN 43.28	AN 54.69	AN 67.82		EN 72.49	EN 42.56	AN 60.45	AN 63.51	FA 30.19	EN 73.64	EN 43.90
WOOD & BANNO C				852					889					859	
WELLS C				814					869					823	

TABLE 1 (continued)

SAMPLE NO	'----------5F-29396A	----------'			'----------7F-29397E			----------'		'----------7G-29400A		----------'	
MINERAL	PL-C	PL-I(*)	OL	OPX	PL-C	PL-I	OL	OPX	CPX	PL-C	OL	OPX	CPX
SIO2	52.97	52.87	38.73	53.97	52.99	52.04	38.21	54.79	52.01	52.53	37.64	53.65	50.65
AL2O3	28.92	29.28	0.01	2.00	29.07	29.92	0.00	1.76	2.81	28.96	0.00	2.48	4.15
TIO2	0.03	0.02	0.02	0.12	0.02	0.01	0.01	0.08	0.52	0.02	0.03	0.21	0.92
FEO(T)	0.15	0.19	27.13	16.50	0.19	0.16	27.18	16.25	6.65	0.18	25.48	15.86	6.36
MNO	0.02	0.07	0.42	0.35	0.01	0.01	0.37	0.38	0.19	0.01	0.33	0.30	0.17
MGO	0.01	0.00	35.80	26.86	0.02	0.00	35.79	27.30	15.64	0.05	35.53	27.34	14.74
CAO	12.44	12.98	0.01	0.55	12.42	13.49	0.02	0.40	22.25	12.40	0.01	0.71	22.20
NA2O	4.24	3.88	0.02	0.02	4.20	3.68	0.02	0.02	0.28	4.11	0.03	0.02	0.46
K2O	0.21	0.20	0.00	0.00	0.30	0.22	0.01	0.00	0.00	0.23	0.01	0.00	0.00
CR2O3	0.01	0.00	0.00	0.01	0.03	0.00	0.02	0.02	0.00	0.02	0.01	0.06	0.10
F	ND				ND	ND				ND			
CL	ND				ND	ND				ND			
TOTAL	98.98	99.49	102.14	100.38	99.25	99.53	101.63	101.00	100.35	98.48	99.07	100.63	99.75
			NUMBERS OF IONS			(*10000)							
	32"O"	32"O"	4"O"	6"O"	32"O'	32"O"	4"O"	6"O"	6"O"	32"O"	4"O"	6"O"	6"O"
SI	96942	96364	10064	19459	96784	94974	9997	19581	19155	96632	10042	19263	18782
AL4+	62376	62908		541	62572	64392	64	419	845	62784	0	737	1218
AL6+			3	309			7	323	374		0	315	593
TI	36	28	4	32	28	8	2	21	144	24	6	55	256
FE2+	228	284	5896	4975	284	241	5947	4856	2048	274	5685	4763	1972
MN	22	116	92	0	12	16	82	0	59	20	75	90	53
MG	36	0	13865	14435	56	9	13956	14542	8585	138	14129	14629	8149
CA	24382	25344	3	212	24312	26394	6	153	8780	24436	3	272	8819
NA	15058	13716	11	14	14860	13009	10	14	199	14670	16	15	329
K	488	464	4	1	696	509	3	1	1	524	3	2	4
CR	10	0	11	2	40	0	4	1	1	18	2	17	30
F	—				—	—				—			
CL	—				—	—				—			
TOTAL	199578	199224	29953	39980	199644	199552	30078	39911	40191	199520	29961	40158	40205
	OR 1.23	OR 1.18		WO 1.08	OR 1.75	OR 1.27		WO 0.78	WO 45.22	OR 1.33		WO 1.38	WO 46.43
	AB 37.72	AB 34.70	FO 70.26	FS 25.35	AB 37.28	AB 32.59	FO 69.84	FS 24.84	FS 10.55	AB 37.00	FO 71.04	FS 24.57	FS 10.66
	AN 61.06	AN 64.12	FA 29.74	EN 73.56	AN 60.97	AN 66.13	FA 30.16	EN 74.37	EN 44.22	AN 61.68	FA 28.96	EN 74.06	EN 42.90
WOOD & BANNO C								933				905	
WELLS C								920				879	

'----------	----------	2G-29301	----------	----------'
PL-C	PL-I	OL	OPX	CPX
52.80	49.98	38.24	53.75	49.95
28.98	30.69	0.03	2.04	4.11
0.04	0.01	0.00	0.07	0.83
0.16	0.19	27.50	16.39	7.13
0.02	0.03	0.31	0.33	0.17
0.01	0.11	36.02	27.25	14.74
12.32	14.35	0.02	0.37	21.73
4.31	3.11	0.02	0.03	0.44
0.25	0.16	0.00	0.01	0.01
0.01	0.01	0.01	0.01	0.02
0.01	0.03			
0.00	0.00			
98.89	98.67	102.15	100.23	99.13
32"O"	32"O"	4"O"	6"O"	6"O"
96772	92391	9962	19399	18709
62597	66865	8	601	1291
			267	520
52	23	1	19	234
243	318	5991	4944	2230
25	43	69	101	53
20	311	13985	14659	8222
24191	28421	5	143	8723
15296	11137	8	18	317
585	365	1	3	2
11	17	3	2	4
76	155			
4	8			
199872	200054	30033	40154	40304
OR 1.46	OR 0.91		WO 0.72	WO 45.38
AB 38.16	AB 27.89	FO 69.77	FS 25.42	FS 11.88
AN 60.38	AN 71.19	FA 30.23	EN 73.87	EN 42.76
			912	
			894	

Pl-C: cumulus plagioclase; Pl-I: intercumulus plagioclase;
Pl-I*: cores of grains
Temperatures (in ±°C) calculated from the thermometers of Wood & Banno, and Wells.

The various lithologies of the St-Henri-de-Taillon segment share the following petrographic characteristics: on an altered surface, the rocks are pale grey, but where fresh they are black. Generally they are plagioclase cumulates, and the plagioclase, depending on rock type, may vary in size from <1 cm to 50–70 cm across. The very coarse-grained plagioclase occurs in the anorthosite, whereas in the leucotroctolite (troctolite), the plagioclase is generally smaller (1 to 5 cm). Late crystallization of the mafic minerals has produced a subophitic or ophitic texture and, less commonly, oikocrysts. If classified according to percentage of postcumulus material (Irvine 1982), the rock types range from plagioclase adcumulates (0–7%) to plagioclase mesocumulates (7–25%). Some plagioclase (-olivine) orthocumulates (25–50%) also are observed, but they are not common. These percentages may be skewed because adcumulus growth around the plagioclase cannot be identified either with the microscope or the microprobe.

The intercumulus mineralogy of the rocks is simple; where the content of mafic minerals is high (>10%), near-cotectic crystallization of intercumulus phases is clearly evident. Six intercumulus minerals are always present. In order of decreasing abundance, these minerals (see Table 1 for details) are: zoned plagioclase more calcic than the cumulus plagioclase, olivine, orthopyroxene, clinopyroxene, oxide (Ti-rich magnetite with exsolved spinel and ilmenite) and apatite. Traces of brown hornblende and biotite appear as spotty overgrowths on mafic minerals. Al-rich orthopyroxene megacrysts (6–8% Al_2O_3) with plagioclase lamellae are locally observed in all lithologies; these megacrysts correspond to Emslie's (1975) type-1 megacryst.

Petrography and Mineralogy

A set of 11 samples has been selected to illustrate a composite cross-section of the St-Henri-de-Taillon segment (Fig. 2, traverses AA′, BB′). Special care was taken to select specimens without mesoscopic traces of deformation, and with minimal recrystallization or alteration visible under the microscope. The sample selection was made to reflect predefor-

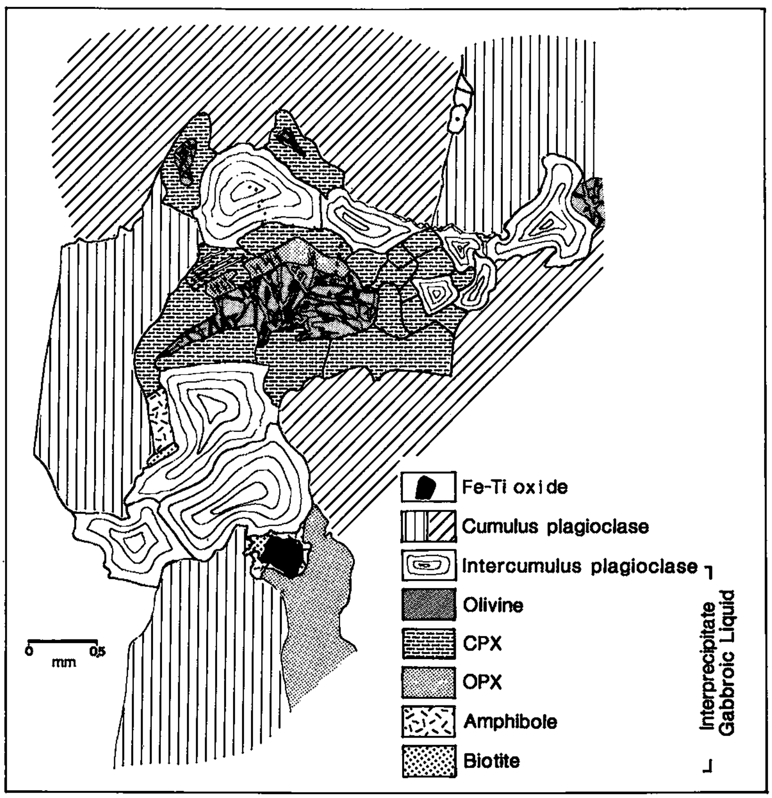

FIG. 4. Schematic representation of the texture of the trapped gabbroic liquid between cumulus plagioclase crystals (drawn from a thin section).

mation characteristics of the rocks.

The rock types investigated are leucotroctolite and anorthosite, with plagioclase as the only cumulus phase. The texture of the intercumulus mineralogical assemblages (olivine gabbro) shows that the corresponding intercumulus liquid was close to a cotectic plagioclase–olivine curve (see Fig. 4). Compositionally, this trapped liquid strongly resembles the leucotroctolitic–troctolitic ovoidal pockets previously described. This is a clear indication that this texture can be observed at various scales.

The compositions of the main minerals were determined at McGill University with an automated Cameca microprobe. An accelerating potential of 15 kV and an emission current of 7 nA were standard conditions. Data were corrected on-line for atomic number, fluorescence and absorption effects according to the ZAF procedure and referred to a suite of synthetic and natural standards. In general, for homogeneous unknown minerals, 3 to 5 spot analyses (1-μm beam) were performed on a single grain and averaged. At least 3 grains of the same mineral were measured per sample. For plagioclase, which locally is optically zoned, at least 5 spot analyses with a 5-μm beam were performed from the center to rim of the grains.

For the two traverses (Fig. 2), a plot of the average compositions *versus* their vertical stratigraphic position showed no evidence of cryptic layering. Only slight local chemical variations were registered in the cumulus plagioclase and in the intercumulus minerals.

Plagioclase

Three different types of plagioclase are evident microscopically: cumulus plagioclase, intercumulus plagioclase and recrystallized plagioclase. They show significant chemical differences (Table 1, Figs. 5, 6).

Plagioclase, the only cumulus mineral in the samples, has not retained a tabular shape except where in contact with mafic minerals. Only rare examples of normal zoning have been observed, but lack of recognition of adcumulus growth prevented distinction between primocrysts and postcumulus overgrowth. Possibly the adcumulus rims were partly or totally blurred by internal strain or by diffusion. At the scale of a thin section the highly strained state of some of the grains is indicated by warped, bent or, in some cases, kinked crystals. Despite the absence of observable adcumulus growth, significant amounts of plagioclase may have been produced by

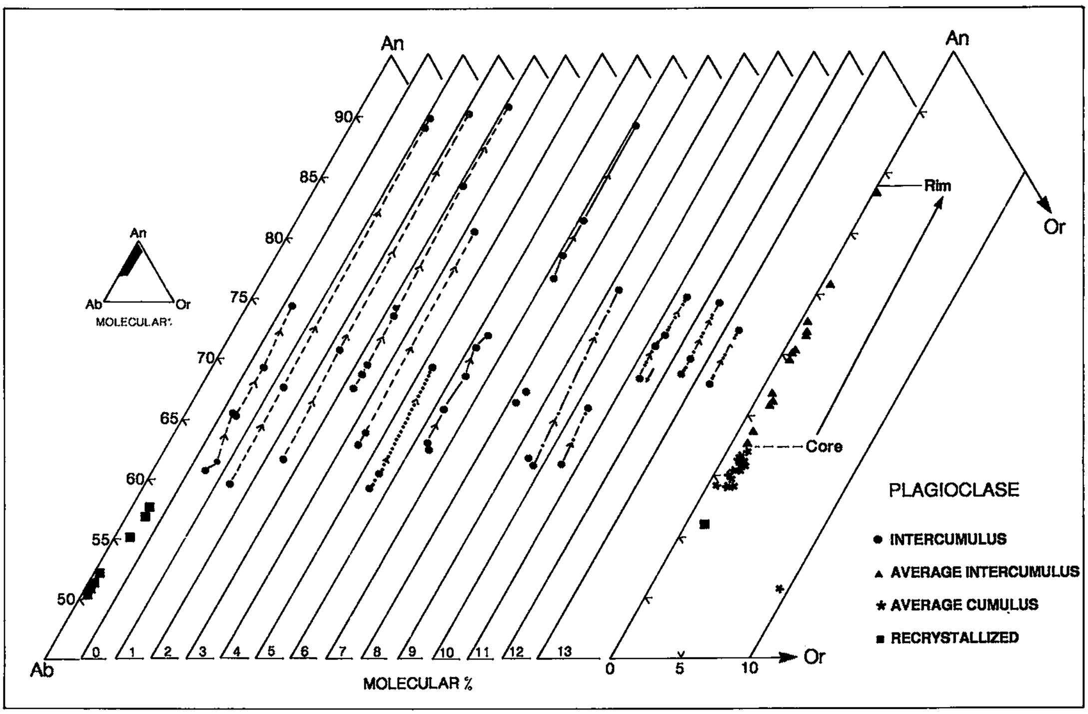

FIG. 5. Ranges of composition of plagioclase in terms of An, Ab and Or, in samples from the St-Henri-de-Taillon sector of the LSJA.

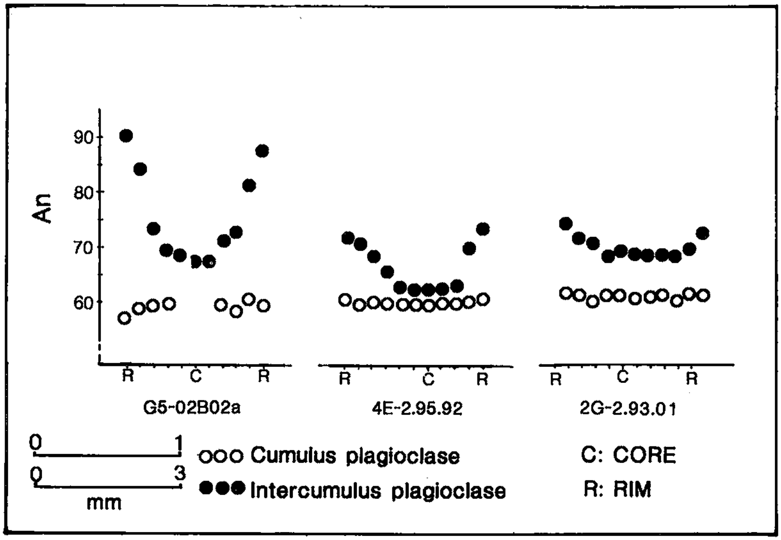

FIG. 6. Schematic plot showing the chemical differences between intercumulus plagioclase and cumulus plagioclase in three crystals (scale is approximate).

such a process, particularly in plagioclase-rich fractions of the rocks.

A second generation of reversely zoned primary plagioclase, which commonly occurs in the intercumulus spaces, is approximately 10 to 15 times smaller in size than the 1- to 3-cm cumulus crystals. The pattern of zoning and smaller size of second-generation plagioclase distinguish it from the larger, optically homogeneous cumulus plagioclase (Figs. 4,5,6).

Secondary plagioclase derived by recrystallization of the primary phase is not common because sample selection was strongly biased in favor of the least recrystallized specimens. However, one slightly deformed sample was retained and analyzed for comparison. At the scale of a thin section, recrystallization of the plagioclase began with the development of thin zones of polygonized grains at the border of cumulus crystals; heterogeneous deformation locally produced a mortar texture. Recrystallized plagioclase is easily distinguished from the others by its small size, its optical homogeneity, and triple-point contacts among the grains.

The composition of cumulus plagioclase is nearly constant from core to margin (*e.g.*, An_{59} to An_{62}; Fig. 6). In each grain, the interval of values is within the range of analytical uncertainty and presumably representative of the original primocryst composition. The An content increases slightly (to An_{65}) in a zone 100 to 150 μm in width, where the cumulus plagioclase is in contact with intercumulus plagioclase which, as described below, has a more calcic rim.

The core of the intercumulus plagioclase has an average composition between An_{59} to An_{65}, which is not significantly higher than that of the cumulus crystals. The grains are reversely zoned; the outer shell, which accounts for approximately half of the volume, shows a sharp increase of 10 to 30 mole % compared to the relatively homogeneous core (Figs. 4,5,6). The difference in chemical composition between cumulus and intercumulus plagioclase of three representative crystals from different stratigraphic levels is presented in Figures 5 and 6.

The recrystallized (*i.e.*, granoblastic) plagioclase has a lower An content (An_{50-52}) than the undeformed plagioclase (An_{60-70}). As only one deformed sample was analyzed (Fig. 5), it is not definite that the drop in An content represents a thin-section, mesoscopic or regional-scale phenomenon.

Olivine

Olivine is the second most abundant mineral. As an intercumulus phase, the olivine ($\sim Fo_{60}$) is locally surrounded by generally unrecrystallized, nonradial partial rims (0.1 to 0.3 mm in width) of orthopyroxene, clinopyroxene, or both. There is no evidence of subsolidus reaction between olivine and plagioclase. Results of the microprobe analysis of coexisting intercumulus olivine and two pyroxenes are presented in Table 1.

Another texture commonly noted is the local development of a thin partial (or, rarely, complete) corona (50 to 100 μm in width) that consists of an inner shell of radial crystals of orthopyroxene and

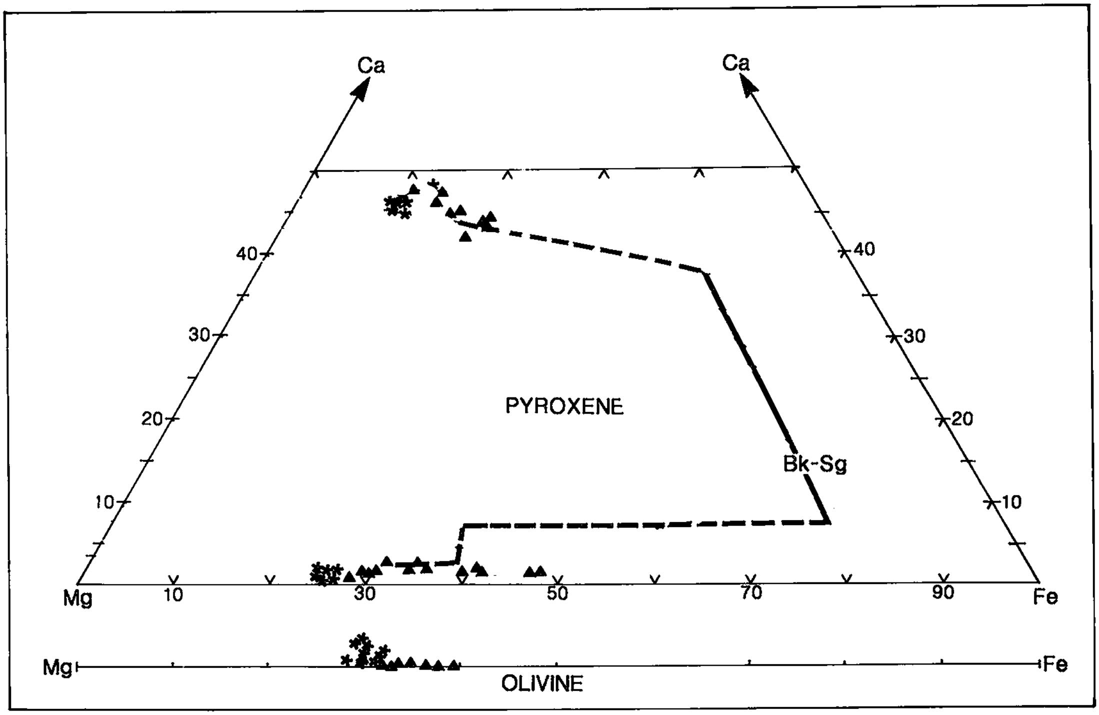

FIG. 7. Plot of pyroxene pairs and of olivine from the St-Henri-de-Taillon (triangle) and Harp Lake (star) complexes. Bj-Sg: trend in the Bjerkrem–Sogndal lopolith (Duchesne 1972).

an outer shell of radial lath of pale green gedrite $(Na_{0.69}Ca_{0.01})(Fe^{2+}_{1.88}Mg_{3.86}Mn_{0.05}Ti_{0.01})(Al_{1.04})(Si_{6.18}Al_{1.82})O_{22}(OH_2)$.

Pyroxenes

Orthopyroxene and clinopyroxene are less abundant than olivine, and commonly form a partial rim around it (Fig. 4). In a few samples, the pyroxenes are intergrown with plagioclase crystals in a subophitic texture. However, the presence of orthopyroxene around olivine may locally indicate a peritectic reaction with the intercumulus liquid. Micrometer-size exsolution lamellae in the clinopyroxene illustrate the retention of the magmatic texture (Jaffe *et al.* 1975).

The compositions of the pairs clinopyroxene ($\sim Wo_{45}$–En_{45}) – orthopyroxene ($\sim En_{72}$) that surround the olivine crystals are plotted (Fig. 7) in the pyroxene quadrilateral. These points do not plot on the crystallization trend for the "Grenville anorthosites and related rocks", as defined by Bohlen & Essene (1978), because the pyroxenes are not corrected for the effects of exsolution; they best fit a wider solvus (Fig. 7) approximately defined by the pyroxenes of the undeformed Harp Lake complex of the Nain Province and the Bjerkrem–Sogndal lopolith of the Dalslandian Province of Norway (Duchesne 1972, Emslie 1980).

Temperatures calculated using 19 pairs of pyroxenes yield an average of 882 ± 37°C (Wood & Banno 1973) and 857° ± 49°C (Wells 1977). These temperatures are intermediate between metamorphic and magmatic conditions, taking into account that the accuracy of these geothermometers is approximately ± 70°C within the calibrated range. Lindsley's geothermometer (Lindsley 1983, Lindsley & Andersen 1983) could not be applied because the percentage of cations other than Fe, Mg and Ca in our compositions exceeds the normal values for a projection in the pyroxene quadrilateral.

DISCUSSION

The St-Henri-de-Taillon segment of the LSJA massif has a transect, 10 km in length, of nearly undeformed anorthositic–leucotroctolitic layered rocks. As indicated by the structures and textures of the rocks, the plagioclase-rich composition of these rocks resulted from concentration by mechanical and chemical processes. Therefore, the volume of magma from which these minerals were derived must have been very large. Direct and indirect evidence tends to single out a basaltic magma as the main source for the genesis of anorthosite massifs (see the reviews by Emslie 1978, 1985, Morse 1982, Duchesne 1984). In the Lac-St-Jean area, the only field evidence of abundant mantle-derived magma is provided by the metabasaltic–metadioritic dykes (amphibolite II dykes; Woussen *et al.* 1981, 1986). These dykes intruded the gneiss complex, predate the emplacement of the LSJA massif, and have a large regional extent. The dykes, which characterize the central and northeastern Core Zone of the Grenville Province, clearly indicate a post-Hudsonian and pre-Grenvillian extensional event (Woussen *et al.* 1981, 1986, Dimroth *et al.* 1981, Owen 1982). The regional abundance and composition of the amphibolite II dyke-swarms are considered to be evidence that the dykes possibly had the same magmatic source as that from which the LSJA massif was derived. If this hypothesis is correct, the problem of how to enrich basaltic magmas sufficiently strongly in aluminum in order to extract the proper amount of plagioclase to form "massif anorthosites" still remains (Emslie 1978, 1985, Morse 1982).

Our detailed analysis of the petrography and mineralogy of the rocks of the St-Henri-de-Taillon area addresses four types of problems related to this layered sequence.

High An content of plagioclase

The plagioclase in anorthosite massifs of the Grenville Province has been reported to range in composition from An_{23} to An_{63} (Anderson & Morin 1969), but Morse (1972) has reported values from An_{40} to An_{80} in the Nain massif. Therefore, we agree with Romey (1968) that the distinction between layered anorthosite massifs, particularly those of the Grenville Province, and the stratiform complexes of the upper crust (*e.g.*, Skaergaard) based on An content of plagioclase is tenuous. Probably a gradation in conditions of formation exists between these two types of intrusive bodies.

Constancy of plagioclase compositions and large volume of cumulus plagioclase

Basaltic magma ponded at the crust–mantle interface precipitated mafic phases, and became progressively enriched in plagioclase components (Emslie 1978, 1985). Because of a cotectic shift toward plagioclase at increased pressures, the magma, upon rising into the crust, was in the plagioclase field until the olivine–plagioclase cotectic was reached at lower pressure. Because of isothermal growth of the phenocrysts during the rise of the magma, this mechanism may explain the large size of the plagioclase crystals and their near-constant composition.

The near-cotectic composition of the cumulus plagioclase–olivine pairs

The mechanism stated above also accounts for the near-cotectic proportion of olivine and plagioclase in the channelways between cumulus plagioclase. Cotectic conditions could have been attained when the magma, laden with plagioclase crystals, settled under conditions of near-constant pressure.

Strong reverse zoning of the intercumulus plagioclase

The origin of reverse zoning in cumulus or intercumulus plagioclase is still debated. Dymek & Gromet (1984) proposed that reverse zoning in intercumulus plagioclase resulted from decomposition of components contained in orthopyroxene. As orthopyroxene is a very minor phase in our rocks, this hypothesis does not explain the observed texture. Morse & Nolan (1984) rejected the possibility of subsolidus reaction(s) and argued that the reversal may develop during intercumulus growth, as the partition coefficient of the An component between plagioclase crystals and liquid is known to increase with the augite component of the trapped liquid. If augite is present in the rocks, which is the case in 90% of our samples (Fig. 4), this mechanism seems to be the most plausible.

As to the subsolidus evolution of the rocks, the temperatures indicated by the Wood & Banno and Wells geothermometers compare with those obtained for the Morin anorthosite (J. Martignole, unpubl. data), the Bjerkrem–Sogndal lopolith (Rietmeijer & Champness 1982), and the Egersund–Ogna anorthosite (Maquil & Duchesne 1984). These temperatures probably reflect a common type of subsolidus evolution even if the absolute values of the temperatures may not be reliable. It is stressed that some of the rocks have been considerably modified by subsolidus recrystallization, by deformation, or both. The most conspicuous effect of alteration is the development, common in olivine-rich layers, of an orthopyroxene–amphibole corona having an outer shell of spinel–quartz symplectite. However, whether these textures originated by prograde regional metamorphism or retrograde, more or less isobaric cooling, is not known.

Conclusions

The following conclusions can be drawn from this study: 1. The St-Henri-de-Taillon segment of the LSJA massif, anorthositic–leucotroctolitic in composition, originated by cumulus processes.
2. The absence of a significant trend, either in oli-

vine or pyroxene compositions, shows that the St-Henri-de-Taillon area probably represents a minor section through an enormous layered mass resulting from the intrusion of several pulses of magma.

3. Large crystals of cumulus plagioclase of near-constant composition grew from a liquid with near-cotectic proportions of plagioclase and olivine. This texture may have resulted from the ascent of a cotectic leucogabbroic magma enriched in plagioclase. Owing to the shift of the cotectic line of the plagioclase – mafic minerals at high pressure, decompression caused protracted precipitation of the plagioclase. When the conditions became nearly isobaric, cotectic crystallization of plagioclase and olivine followed.

4. Strong reverse zoning in the intercumulus plagioclase is best explained by the Morse–Nolan hypothesis.

5. The segment of the LSJA described here shares more features with layered complexes than with the ill-defined "massif-type" of anorthosite.

Acknowledgements

The comments of E.H. Chown, R.F. Dymek and R.F. Emslie greatly helped to improve preliminary versions of the manuscript. We acknowledge the helpful reviews of R.F. Martin, S.A. Morse, A.R. Philpotts and S.J. Barnes. Field work was carried under the auspices of the MER of Quebec. Part of this research was supported by research grants A 7058 to JM and A 8444 to GW.

References

ANDERSON, A.T., JR. & MORIN, M. (1969): Two types of massif anorthosites and their implications regarding the thermal history of the crust. *In* Origin of Anorthosites and Related Rocks (Y.W. Isachsen, ed.). *N.Y. State Mus. Sci. Serv., Mem.* **18**, 57–69.

BENOIT, F.W. & VALIQUETTE, G. (1971): Région du Lac-St-Jean (partie sud), Québec. *Ministère des Richesses Naturelles du Québec, Rapp. Géol.* **140**.

BOHLEN, S.R. & ESSENE, E.J. (1978): Igneous pyroxenes from metamorphosed anorthosite massifs. *Contr. Mineral. Petrology* **65**, 433–442.

DE WAARD, D. & ROMEY, W.D. (1969): Petrogenetic relationships in the anorthosite–charnockite series of Snowy Mountain Dome, south central Adirondacks. *In* Origin of Anorthosites and Related Rocks (Y.W. Isachsen, ed.). *N.Y. State Mus. Sci. Serv., Mem.* **18**, 307-315.

DIMROTH, E., WOUSSEN, G. & ROY, D.W. (1981): Geological history of the Saguenay region, Quebec (Central Granulite Terrain): a working hypothesis. *Can. J. Earth Sci.* **18**, 1506-1522.

DUCHESNE, J.-C. (1972): Pyroxènes et olivines dans le massif de Bjerkrem–Sogndal (Norvège méridionale). Contribution à l'étude de la série anorthosite–mangérite. *24th Int. Geol. Congress* (Montreal) **2**, 320-328.

______ (1984): Massif anorthosites: another partisan review. *In* Feldspars and Feldspathoids (W.L. Brown, ed.). D. Reidel Publishing Co., Dordrecht, Holland.

DYMEK, R.F. & GROMET, L.P. (1984): Nature and origin of orthopyroxene megacrysts from the St-Urbain anorthosite massif, Quebec. *Can. Mineral.* **22**, 297-326.

EMSLIE, R.F. (1975): Pyroxene megacrysts from anorthositic rocks: new clues to the source and evolution to the parent magma. *Can. Mineral.* **13**, 138-145.

______ (1978): Anorthosite massifs, rapakivi granites and late Proterozoic rifting of North America. *Precamb. Res.* **7**, 61-98.

______ (1980): Geology and petrology of the Harp Lake complex: an example of Elsonian magmatism. *Geol. Surv. Can. Bull.* **293**.

______ (1985): Proterozoic anorthosite massifs. *In* The Deep Proterozoic Crust in the North Atlantic Provinces (A.C. Tobi & J.L.R. Touret, eds.). *Proc. NATO Adv. Study Inst., Ser.* **C158**, 39-60.

GRAVITY DIVISION, ENERGY, MINES AND RESOURCES CANADA (1974): Bouguer anomaly map of Canada. *Earth Phys. Branch, Energy Mines & Resources, Gravity Map ser.* **74–1**.

HOCQ, M. (1977): *Contribution à la Connaissance Pétrotectonique et Minéralogique des Massifs Anorthositiques et Mangéritiques de la Région du Réservoir Pipmuacan.* Ph.D. thesis, Univ. Montréal, Montréal, Québec.

IRVINE, T.N. (1982): Terminology for layered intrusions. *J. Petrology* **23**, 127-162.

JACKSON, E.D. (1967): Ultramafic cumulates in the Stillwater, Great Dyke and Bushveld intrusions. *In* Ultramafic and Related Rocks (P.J. Wyllie, ed.). John Wiley & Sons, New York.

JAFFE, H.W., JAFFE, E.B. & ROSS, M. (1975): Orientation of pigeonite exsolution lamellae in metamorphic augite: correlation with composition and calculated optimal phase boundaries. *Amer. Mineral.* **71**, 773-75.

KEHLENBECK, M.M. (1972a): Deformation textures in the Lac Rouvray anorthosite mass, Quebec. *Can. J. Earth Sci.* **9**, 1087-1098.

______ (1972b): Tectonic evolution of the Lac Rouvray anorthosite mass. *Can. J. Earth Sci.* **9**, 1640-1649.

LAURIN, A.F. & SHARMA, K.N.M. (1975): Mistassini, Peribonka, Saguenay rivers area (Grenville 1965-1967). *Quebec Dep. Nat. Resources, Geol. Rep.* **161.**

LINDSLEY, D.H. (1983): Pyroxene thermometry. *Amer. Mineral.* **68**, 477-493.

______ & ANDERSEN, D.J. (1983): A two-pyroxene thermometer. *J. Geophys. Res.* **88** (suppl., part 2), A887-A906.

MAQUIL, R. & DUCHESNE, J.-C. (1984): Géothermométrie par les pyroxènes et mise en place du massif anorthositique d'Egersund-Ogna (Rogaland, Norvège méridionale). *Ann. Soc. Géol. Belg.* **107**, 27-49.

MCCALLUM, I.S., RAEDEKE, L.D. & MATHEZ, E.A. (1980): Investigations of the Stillwater Complex. I. Stratigraphy and structure of the banded zone. *Amer. J. Sci.* **280-A**, 59-87.

MICHOT, J. & MICHOT, P. (1969): The problem of anorthosite: the South Rogaland igneous complex, southwestern Norway. *In* Origin of Anorthosite and Related Rocks (Y.M. Isachsen, ed.). *N.Y. State Mus. Sci. Serv., Mem.* **18**, 399-423.

MORSE, S.A. (1972): Plagioclase composition variation. *In* The Nain Anorthosite Project, Labrador: field report 1972 (S.A. Morse, ed.). *Contr. Univ. Massachussetts* **11**, 103-116.

______ (1982): A partisan review of Proterozoic anorthosites. *Amer. Mineral.* **67**, 1087-1100.

______, NOLAN, K.M. (1984): Origin of strongly reversed rims on plagioclase in cumulates. *Earth Planet. Sci. Lett.* **68**, 485-498.

NANTEL, S., MARTIGNOLE, J. & WOUSSEN, G. (1985): Géologie et zones potentielles pour l'exploitation de la pierre de taille. Partie sud-ouest du massif d'anorthosite du Lac-St-Jean. *Ministère Energie Ressources Québec, rapp. final.* **ET-83-17.**

OWEN, J.V. (1982): *Petrography of Leucocratric Segregations in the Migmatitic Old Gneiss Complex East of Chicoutimi, Québec.* M.Sc. thesis, Univ. du Québec à Chicoutimi, Chicoutimi, Québec.

RIETMEIJER, F.J.M. & CHAMPNESS, P.E. (1982): Exsolution structures in calcic pyroxenes from the Bjerkrem-Sogndal lopolith, SW Norway. *Mineral. Mag.* **45**, 11-24.

RIVERS, C.T., MARTIGNOLE, J., GOWER, C. & DAVIDSON, A. (1988): A new subdivision of the Grenville Province. *Tectonics.*

ROMEY, W.D. (1968): An evaluation of some "differences" between anorthosite in massif and in layered complexes. *Lithos* **1**, 230-241.

ROY, D.W., WOUSSEN, G., DIMROTH, E. & CHOWN, E.H. (1986): The Central Grenville Province: a zone of protracted overlap between crustal and mantle processes. *In* New Perspectives on the Grenville Province (J.A. Moore & A. Davidson, eds.). *Geol. Assoc. Can., Spec. Pap.* **31**, 51-60.

WELLS, P.R.A. (1977): Pyroxene thermometry in simple and complex systems. *Contr. Mineral. Petrology* **62**, 129-139.

WOOD, B.J. & BANNO, S. (1973): Garnet–orthopyroxene and orthopyroxene–clinopyroxene relationships in simple and complex systems. *Contr. Mineral. Petrology* **42**, 109-124.

WOUSSEN, G., DIMROTH, E., CORRIVEAU, L. & ARCHER, P. (1981): Crystallization and emplacement of the Lac-St-Jean anorthosite massif (Quebec, Canada). *Contr. Mineral. Petrology* **76**, 343-350.

______, ROY, D.W., DIMROTH, E. & CHOWN, E.H. (1986): Mid-Proterozoic extensional tectonics in the Core Zone of the Grenville Province. *In* New Perspectives on the Grenville Province (J.A. Moore & A. Davidson, eds.). *Geol. Assoc. Can., Spec. Pap.* **31**, 297-311.

Received November 26, 1986, revised manuscript accepted January 24, 1988.